Ultra-high speed and ultra-high resolution spectral-domain optical coherence tomography and optical doppler tomography in ophthalmology

CENSE B.[1], CHEN T.C.[2], NASSIF N.[1], PIERCE M.C.[1], YUN S.H.[1], PARK B.H.[1], BOUMA B.E.[1], TEARNEY G.J.[1], DE BOER J.F.[1]

ABSTRACT

We present ultra-high resolution optical coherence tomography (OCT) structural intensity and optical Doppler tomography (ODT) flow velocity images of the human retina in vivo. The ultra-high speed OCT system is based on Spectral Domain or Fourier Domain technology, which provides a sensitivity advantage over conventional OCT of more than 2 orders of magnitude. This sensitivity improvement allows video rate OCT and ODT cross sectional imaging of retinal structures. Images will be presented with axial resolutions of 6 and 3.5 microns. We observed small features in the inner and outer plexiform layers, which are believed to be small blood vessels. Flow velocity images will be presented showing pulsatile flow in retinal arteries and veins.

KEYWORDS

Optical Coherence Tomography, Spectral Domain OCT, Fourier domain OCT, Doppler Optical Coherence Tomography, Anterior segment imaging, Retinal blood flow

RÉSUMÉ

Nous présentons des images de intensité structurelle par tomographie par cohérence optique (TCO) à ultra-haute résolution et de vitesse de flux sanguin par tomographie Doppler optique (TDO) de la rétine humaine in vivo. Le système TCO à ultra-haute vitesse est basé sur la technologie en Domaine Spectral ou en Domaine Fourier, qui possède un avantage de sensibilité par rapport à une TCO conventionnelle de plus de 2 ordres de magnitude. Cette amélioration de sensibilité permet une imagerie transversale par TCO et TDO à fréquence vidéo des structures rétiniennes. Les images seront présentées avec une résolution axiale de 6 et 3,5 microns. Nous avons observé de petits éléments dans les couches plexiformes internes et externes, que l'on pense être de petits vaisseaux sanguins. Les images de la vitesse de flux seront présentées en montrant le flux pulsatile dans les artères et veines rétiniennes.

MOTS-CLÉS

Tomographie par cohérence optique à ultra-haute résolution, tomographie Doppler optique, TCO en domaine spectral, TCO en domaine Fourier, flux sanguin, TCO en domaine temporel

.....

[1] *Harvard Medical School and Wellman Center for Photomedicine, Massachusetts General Hospital, Boston, MA*
[2] *Massachusetts Eye and Ear Infirmary and Harvard Medical School, Boston, MA*

INTRODUCTION

Optical Coherence Tomography (OCT) was introduced in the early 1990s. Based on interferometry with near infrared light, OCT allows for non-invasive and in vivo optical cross-sectioning of the retina and cornea. In OCT, the reference arm of a Michelson interferometer is rapidly scanned over the cross-sectional imaging depth (Fig. 1). This technique is now generally referred to as Time Domain OCT (TDOCT), since an A-scan or depth profile is acquired by scanning a mirror in the reference arm as a function of time. TDOCT is a technique that is clinically applied in ophthalmology for the detection of ocular diseases, as well as for monitoring of disease progression and the effects of therapy.

The lateral resolution of the technique is limited by the optics of the eye, i.e. the focal length, corneal aberrations and pupil diameter,[2] and the optical design of the setup. Without adaptive optics, the combination of these parameters leads to a lateral resolution of approximately 20-30 μm. The axial resolution of an OCT system may be defined in terms of the coherence length, l_{coh}, which is determined by the center wavelength and bandwidth of the source and the index of refraction of the medium.[22] Drexler et al obtained retinal images with an axial resolution of 3 μm,[10] using a technique called ultra-high resolution optical coherence tomography (UHROCT).[8-10]

The image quality or signal to noise ratio (SNR) of an OCT system is ultimately limited by shot noise, which is a fundamental noise component related to the discrete (particle) nature of light. The best performance of an OCT system is achieved when the SNR is limited by shot noise. The SNR of such a shot-noise-limited TDOCT system depends on several factors.[22] The use of a source with a larger bandwidth increases axial resolution, but decreases SNR due to the increased electronic detection bandwidth required. In order to maintain the same SNR, either A-line rate or axial scan length should be decreased, or the power incident on the sample should be increased. If the dwell time of the imaging spot on the retina is kept short, ANSI standards allow an increase of sample power.[1] Short dwell times can be achieved if the OCT beam is scanned sufficiently fast over the retina. Hitzenberger et al performed ophthalmic TDOCT with short dwell times and incident power of up to 10 mW.[14] In previous measurements with our ophthalmic TDOCT system, the power incident on the eye was less than 600 μW,[3] because this power level is known to be safe for dwell times of up to eight hours.[1] An increase in sample arm power to 10 mW could result in more than a tenfold increase in SNR. However, more source power is required and a scanner failure would lead to a retinal exposure exceeding the ANSI standards. For current clinical ophthalmic applications of UHROCT, either a lower SNR or a slower A-line rate is taken as a penalty. One can avoid such a penalty by using a more sensitive technique.

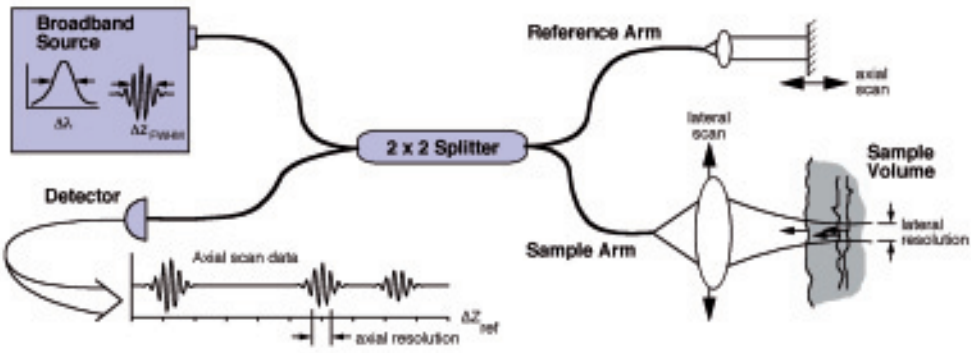

Fig. 1. Typical configuration of a Time Domain OCT system. The reference arm is rapidly scanned and produces interference fringes when the sample and reference arm length are matched. In this example, three reflective structures in the sample arm are shown. In the detection arm, three fringe patterns are detected when the reference arm length is scanned and the length matches to the structures in the sample arm.

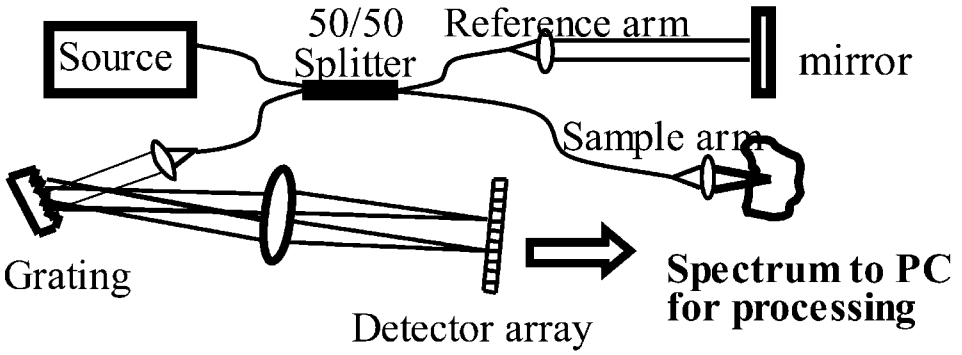

Fig. 2. Typical configuration of a Spectral Domain OCT system. The reference arm does not require mechanical scanning. In the detection arm, a spectrometer measures the spectrum. Depth information is retrieved by a Fourier transform of this spectrum.

In spectral-domain optical coherence tomography (SDOCT), also known as Fourier-domain OCT (FD-OCT), depth-resolved information is acquired by measuring the spectrum in the detection arm of the interferometer (Fig. 2).[11-13] A Fourier transformation of the spectrum retrieves the depth information, hence the name Spectral Domain or Fourier Domain OCT. SDOCT offers a significant sensitivity advantage over TDOCT.[6-7,16,18] Recently, in a direct comparison, an improvement of more than 2 orders of magnitude (21.7 dB) was experimentally demonstrated.[20] In addition, the reference arm length in SDOCT does not require a scanning mechanism, which makes SDOCT inherently faster than TDOCT. The SNR of a shot-noise limited SDOCT system is given by:[7]

$$SNR_{SD-OCT} = \frac{\eta \cdot P_{sample} \cdot \tau_i}{E_v} \quad (1)$$

with η the detector Quantum Efficiency, P_{sample} the power reflected from the sample arm, τ_i the integration time required to record one spectrum, and E_v the energy of a single photon. According to equation 1, the SNR performance of an SDOCT system improves with increasing sample arm power or longer integration time. Most importantly, equation 1 shows that the SNR performance of an SDOCT system is independent of the bandwidth of the source. In theory, by combining SDOCT with an ultra-broadband source, ultrahigh-resolution imaging at high acquisition rates should become within reach.

The first in vivo retinal SDOCT images were presented by Wojtkowski et al.[24] In our previous work, we demonstrated an SDOCT system suitable for in vivo video-rate ophthalmic imaging.[19,20] This system had a sensitivity of 98.4 dB, an acquisition rate of 29,300 A-lines per second and an axial resolution of 6 μm in the eye at a safe ocular exposure level of 600 μW. Motion artifacts within a frame due to involuntary eye movement were avoided at this frame rate. Furthermore, three-dimensional tomograms were created, which represent the true topography of the retina. More recently, we demonstrated a system with an ultra-high broadband source resulting in an axial resolution of 3.5 microns, which was confirmed in vivo by measuring the specular reflection of the foveal umbo.[4] This resolution allowed for the first time identification of very small structures in the inner plexiform layer, believed to be small blood vessels.

Spectral domain technology not only offers structural retinal imaging but also allows imaging of retinal blood flow similar to Doppler ultrasound.[25] The flow sensitivity of Doppler OCT greatly depends on the mechanical or phase stability of the OCT system and on how fast images can be taken.[15,27] Due to the dramatic speed improvement of SDOCT and the absence of moving parts in the reference arm, flow sensitivity is greatly improved.[17,23] For SDODT, the measured phase stability of our system was more than 25 times better than previously quantified figures for TDODT

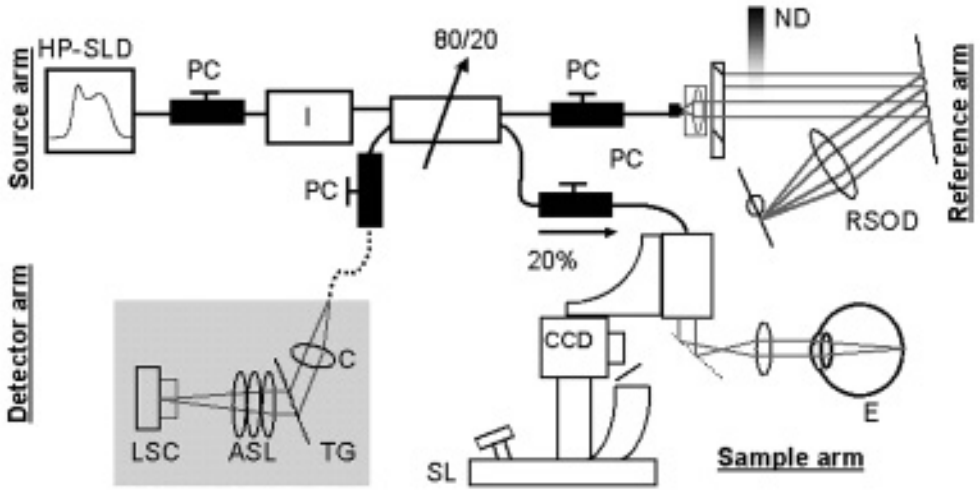

Fig. 3. Schematic of the SDOCT setup that was used for in vivo measurements. HP-SLD: high power superluminescent diode or broadlighter. PC: polarization controllers. ND: neutral density filter. RSOD: delay line; LSC: line scan camera. ASL: air spaced lens. TG: transmission grating. C: collimator. CCD: charge coupled device. E: Eye. SL: slit-lamp.

systems, and at our acquisition speed corresponds to a minimum detectable Doppler shift of ±25 Hz and a dynamic range of 600, defined as the ratio of maximum to minimum detectable Doppler shift.[23] Images were acquired at 29 frames per second (1000 A-lines per frame) and demonstrated pulsatile flow in arteries and veins, blood flow within blood vessels as small as 10 μm and flow as deep as the choroid.[23]

METHOD

A detailed description and drawing of our setup can be found in our earlier work.[4,19-20,23] Two different light sources were employed to generate images with axial resolutions of 6 and 3.5 microns, respectively. The first source was superluminescent diode (HP-SLD371, Superlum, Russia) with 8 mW of power, a central wavelength of 840 nm and full width at half maximum bandwidth (FWHM) of 50 nm. The second source was a BroadLighter (Superlum, Russia), in which two super luminescent diodes at center wavelengths of approximately 840 nm and 920 nm were combined in one system with a center wavelength of 890 nm, a FWHM bandwidth of over 150 nm and an optical output power of approximately 4.5 mW.

Back reflected light from the source was isolated with a broadband isolator. Without the isolator, back reflections induce noise in the OCT system. After isolation, the power was split with a fiber coupler. The splitting ratio of this coupler was optimized to 80/20 at 830 nm. The larger fraction was sent towards a stationary rapid scanning optical delay line, in which the lens-to-grating distance was optimized to minimize group-delay or second order dispersion. The smaller fraction of the power was sent towards the sample arm, where a slit lamp-based scanner apparatus was available for retinal scanning. The power that was incident on the cornea was equal to 395 ± 5 mW. This power is well below the allowed maximum for scanning beams as specified by the ANSI standards.[1] Power returning from the eye and the reference arm interfered in the 80/20 fiber coupler. Interference fringes were detected with a high-speed spectrometer, comprising a collimator (f = 60 mm), a transmission grating (1200 lines/mm) at Littrow's angle, a three-element air-spaced focusing lens (f = 100 mm) and a line scan camera (Basler) with 2048 elements (each 10 μm × 10 μm). The bandwidth of the spectrometer was 145 nm, with a designed spectral resolution equal to 0.071 nm.[19-20] The maximum scan depth z was equal to

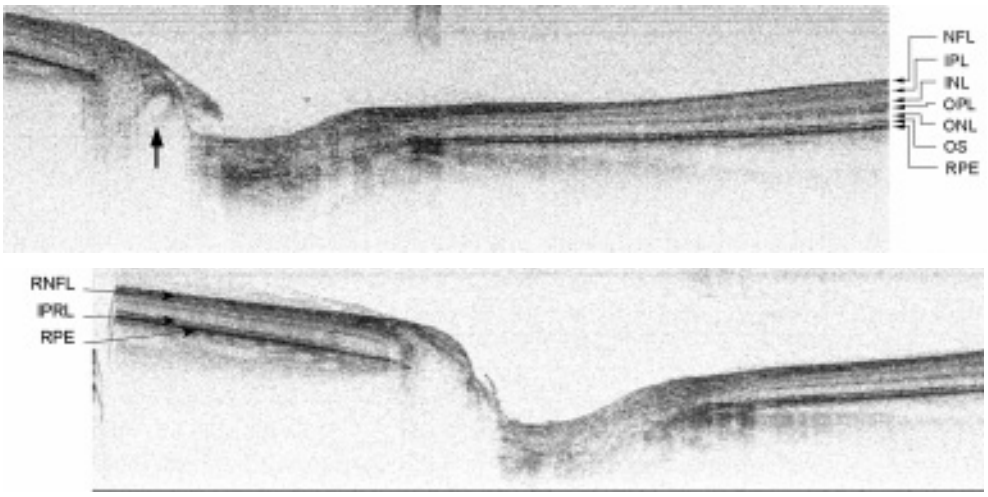

Fig. 4. Two cross sectional images of the optic nerve head of a healthy human volunteer. Image size is 6.4 mm wide by 1.7 mm deep. Images were acquired in 1/30th of a second. Individual layers in the retina are labeled as: NFL - retinal nerve fiber layer; IPL - inner plexiform layer; INL - inner nuclear layer; OPL - outer plexiform layer; ONL - outer nuclear layer; ELM - external limiting membrane; OS - interface between the inner and outer segments of the photoreceptor layer; RPE - retinal pigmented epithelium. In the upper image, an arrow points to a blood vessel. Reprinted from references 20 and 5 with permission from the Optical Society of America and the American Medical Association, respectively.

2.7 mm in air and 2.0 mm in tissue (n = 1.38). In the spectrometer, consecutive interference spectra were read out using a custom-made program written in Visual C++.[19-20] Data was stored on a hard disk. The continuous acquisition rate was 29,300 spectra per second. The integration time per spectrum was equal to 34 μs. The duty cycle was 98 %, i.e. data was acquired during 98 % of the total imaging time.

MEASUREMENT PROCEDURE

In vivo measurements were performed on the undilated right eye of a healthy volunteer. The right eye was stabilized using an external fixation spot for the volunteer's contralateral eye. Multiple sets of B-scans were taken in the macular area at an acquisition rate of 29,300 spectra per second. During acquisition, a refresh rate on screen of three frames per second without dispersion compensation was maintained. For each frame the fast axis of the retinal scanner was deflected once, while the slow axis of the scanner could be stepped between frames.

ANALYSIS

Data was analyzed after acquisition with a custom-made program written in Matlab. Raw data was processed in several steps to extract structural intensity images [19-20,26] as well as Doppler flow data.[23] In addition, we compensated for dispersion in software.[4] Raw data was converted to movies in Matlab as well. Images with a resolution of 6 microns were acquired at an A-line rate of 29,400 per second, resulting in 29 frames per second with 1000 A-lines per frame. For the 3.5 micron resolution images, two consecutive spectra were summed before Fourier transformation to improve SNR. At an effective A-line rate of 14,600 per second, movies of 500 A-lines per frame and 29 frames per second were created. The conversion of a data set acquired in 3 seconds into a movie took approximately twenty minutes in MatLab.

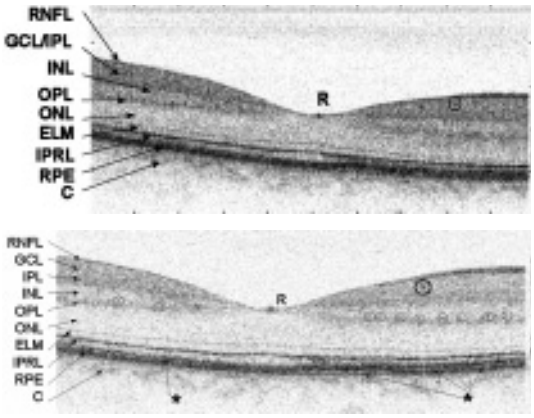

Fig. 5. Structural images of the fovea at nearly identical locations. Top image: 6 micron resolution. Bottom image: 3.5 micron resolution. The image is expanded in the vertical direction by a factor of 2 for clarity. Layers are labeled as follows: RNFL - retinal nerve fiber layer; GCL - ganglion cell layer; IPL - inner plexiform layer; INL - inner nuclear layer; OPL - outer plexiform layer; ONL - outer nuclear layer; ELM - external limiting membrane; IPRL - interface between the inner and outer segments of the photoreceptor layer; RPE - retinal pigmented epithelium; C - choriocapillaris and choroid. A highly reflective spot in the center of the fovea is marked with an R. A blood vessel is marked with a large circle and structures in the outer plexiform layer are marked with smaller circles. Two layers at the location of the RPE at the left and right are marked with arrows and asterisks (*). Reprinted from reference 4 with permission from the Optical Society of America.

RESULTS

In vivo measurements on a human volunteer are presented in figure 4. Two representative frames from different movie sequence centered on the optic nerve head are shown. Each image was 6.4 mm wide by 1.7 mm deep.[19-20] Individual layers of the retina can be clearly distinguished. As the scan moves through the optic nerve head, several blood vessels are seen. Shadows associated with blood vessels are easily seen in the movie, tracking with the vessels entering the optic nerve head.

In figure 5, two images are presented of the fovea with a resolution of 6 microns (top) and 3.5 microns (bottom), acquired with the HP-SLD and the broadlighter, respectively. The movie frames are expanded in vertical direction by a factor 2. The retinal scanner made horizontal scans through the fovea. For this particular data set, the slow axis of the retinal scanner was not run and as a result cross-sections from approximately the same location can be seen as a function of time.[4] Several layers can be recognized in these images.[10] The upper dark band at the left and right of the image is the retinal nerve fiber layer that becomes thicker further away from the fovea. Below this layer, we see two dark bands delineated by two whiter bands. The upper dark band consists of the ganglion cell layer and the inner plexiform layer. In several frames, one may be able to distinguish between these two layers. The two white bands are the inner and outer nuclear layers, and the second dark band is the outer plexiform layer. The first dark layer below the outer nuclear layer is the external limiting membrane, which extends over the whole width of the image. This layer is in general not visible with OCT employed with an ordinary broadband source. Below this membrane we can see the interface between the inner and outer segments of the photoreceptor layer, which rises directly below the foveola. The lowest layer comprises the retinal pigment epithelium (RPE). At the left and right side of the image at the location of the RPE, two layers seem to be present. We hypothesize that one of these layers might be Bruch's membrane. Below the RPE, a cloudy structure can be seen. This structure is the choriocapillaris and the choroid. The fast acquisition rate reveals the true topography of the retina.

In the image with 3.5 micron axial resolution, small highly-reflecting black dots can be seen in the ganglion cell layer and in both plexiform layers. We conclude that they are not caused by

speckle, because they consistently appear at the same location over consecutive movie frames. The dots seem to be almost regularly spaced in the outer plexiform layer. We believe that these black dots are very small blood vessels. Snodderly et al. measured the distribution of blood vessels in an enucleated macaque eye by means of microscopy in frozen samples.[21] They report a very similar spacing of small blood vessels in the plexiform layers near the fovea. To positively identify these structures as blood vessels, we analyzed the data for blood flow as described in our earlier work.[23] Doppler flow analysis confirmed that flow occurs in the darker dots located in the ganglion cell layer, which therefore can be positively identified as blood vessels. In the plexiform layers, a clear correlation between location of the highly reflective black dots and Doppler flow could not be found. Flow was only detected incidentally in these layers at locations where black dots were seen. One explanation that no consistent flow was detected in the well-reflecting features in the plexiform layers is that these features are not blood vessels. Another explanation may be that our system is not sensitive enough to measure flow in such small vessels. For instance, the blood vessels may be too small, which reduces the number of A-lines and therefore the signal that can be used to determine the presence of blood flow. Furthermore, the analysis depends on measuring a Doppler component parallel to the direction of the beam. If the blood vessel is exactly perpendicular to the beam direction, a parallel Doppler flow component will be absent and no flow can be registered. In previous work, larger blood vessels were recognized by their white appearance and the shadow they cast, caused by light attenuation in the blood. Here blood vessels act as good scatterers, presumably due to their small sizes.

OPTICAL DOPPLER TOMOGRAPHY

Images were acquired at 29 frames per second (1000 A-lines per frame) and subsequently processed. Figure 6 shows a single frame out of a movie containing 95 frames acquired in 3.28 seconds of the retina of a healthy volunteer. The pupil was not dilated for these measurements. The upper panel shows the intensity image, while the lower panel shows the bi-directional Doppler flow image. The frames are 1.6 mm wide and have been cropped in depth to 580 μm, from their original size of 1.7 mm. The layers of the retina visible in the intensity image have been identified and described previously, with the thick, uppermost layer being the nerve fiber layer, and the thinner, strongly scattering deep layer being the retinal pigment epithelium. Vessel walls are distinct in the phase image, allowing better determination of vessel size and position than may be obtained by identifying shadows cast in the intensity image. There are many notable features within the image. First, note the artery-vein pair on the left-hand side of the image. As the movie progresses over the period of four heartbeats, one can see the pulsatility of blood flow in the artery (a), while the flow in the vein (v) is less variable.[23] The large blood vessels to the right produce notable shadowing effects due to forward-scattered photons. However, the vessel boundaries are still easily determined in the phase image, and the pulsatile nature of flow is evident in the movie. At the lower left center of the image, it is possible to distinguish blood flow deep within the retina (d). With reference to the intensity image, one can see that this blood flow is being detected below the retinal pigment epithelium, and we believe this is the first time that optical Doppler tomography imaging techniques have been able to observe and localize blood flow within the choroid. To the left of the large vessel on the right-hand side of the image, note the appearance of a very small vessel (c). The diameter of this vessel is slightly under 10 μm (6 pixels by 5 pixels), which is on the same order as the resolution of the system.

The ultra-high speed acquisition time of the SD-ODT system allows determination of pulsatile flow dynamics. The identity of vessels in artery-vein pairs can be distinguished, as flow velocity in arteries varies closely with the cardiac cycle, while the blood flow in veins exhibits less fluctuation and lag in phase.

The retinal blood flow dynamics are further quantified in figure 7. The average Doppler shift has been computed at each instance in time over a box of 160 $\times$ 170 μm that surrounds the small

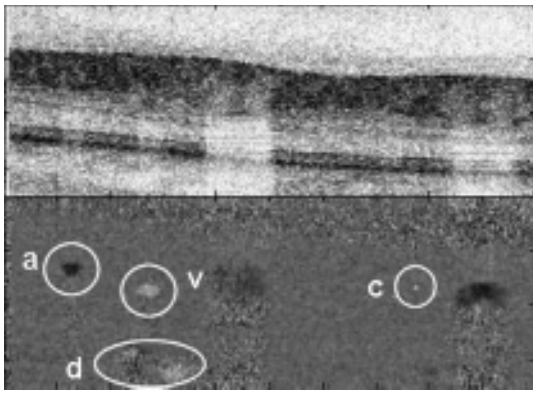

Fig. 6. Movie frame of structure (top panel) and bi-directional flow (bottom panel) acquired in vivo in the human eye at a rate of 29 frames per second. The sequence contained 95 frames (totaling 3.28 seconds). Image size is 1.6 mm wide by 580 μm deep. a: artery; v: vein; c: capillary; d: choroidal vessel. Reprinted from reference 23 with permission of the Optical Society of America.

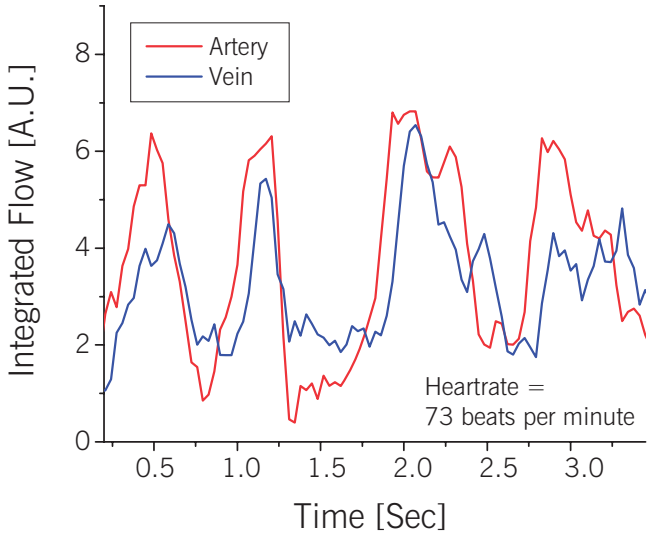

Fig. 7. Integrated flow over the artery-vein pair shown in figure 6. A total of 95 frames were acquired at 29 fps, resulting in a total imaging time of 3.28 s. Reprinted from reference 23 with permission of the Optical Society of America.

(~100 μm diameter) artery on the left-hand side of the image in figure 6. A similar calculation is performed on the adjacent small vein. This average Doppler shift is then graphed over time, with plotted data points representing the mean value from 2 consecutive frames. One can see that flow in the artery follows the expected pulsing pattern. Blood velocity increases rapidly and then slowly decays, repeating four times over 3.28 seconds. Over the same time period, the pulsatile flow effects in the vein are slightly lower and lag in phase with respect to the arterial flow.

CONCLUSIONS

In summary, we have presented the advantage of SDOCT over conventional TDOCT for in vivo human retinal imaging. The ultra-high speed system offers many advantages in retinal imaging,

maintaining high signal to noise while operating at a safe ocular exposure level. SDOCT's higher acquisition speeds realistically allow for a shift from two-dimensional to three-dimensional (3D) images of ocular anatomy.[19] For example, a 6.2 mm by 6.2 mm area with 62 parallel images 100 microns apart can be obtained in 2.1 seconds. Scan areas can be adjusted and scan intervals can be decreased as needed. Motion artifacts within a single image become almost negligible with the ultra-high speed nature of SDOCT. Since patient motion artifacts are more of a problem as people become older, the ultra-high speed nature of SDOCT is particularly helpful since some of the most common causes of blindness increase in prevalence as people age (i.e. glaucoma, age-related macular degeneration, and diabetic retinopathy). With SDODT, vasculature can be accurately situated in true retinal topography. Large cross-sectional images can be made while retaining high resolution that allows the detection of small blood vessels and capillaries of sizes on the order of 10 μm. SDODT also demonstrates the ability to obtain accurate phase information on blood flow from large penetration depths. We were able to detect blood flow below the RPE despite high beam attenuation. The high imaging speed allows detection of pulsatile flow dynamics, distinguishing arteries from veins, and charting velocity throughout a cardiac cycle. We believe these benefits that spectral domain ODT possess will make it a useful investigational and diagnostic tool.

ACKNOWLEDGMENTS

This research was supported in part by a research grants from the National Institutes of Health (1R24 EY12877). Research grants for technical development were provided in part by the National Institute of Health (R01 EY014975 and RR19768), Department of Defense (F4 9620-01-1-0014), CIMIT, and a gift from Dr. and Mrs. J.S. Chen to the optical diagnostics program of the Wellman Center for Photomedicine.

REFERENCES

(1) AMERICAN NATIONAL STANDARDS INSTITUTE – American National Standard for Safe Use of Lasers Z136.1. 2000; National Laser Institute, Orlando FL 2000
(2) CAMPBELL F.W., GREEN D.G. – Optical and Retinal Factors Affecting Visual Resolution. J Physiol London 1965; 181: 576
(3) CENSE B., CHEN T.C., PARK B.H., PIERCE M.C., DE BOER J.F. – In vivo depth-resolved birefringence measurements of the human retinal nerve fiber layer by polarization-sensitive optical coherence tomography. Opt Lett 2002; 27: 1610-1612
(4) CENSE B., NASSIF N.A., CHEN T.C., PIERCE M.C., YUN S.H., PARK B.H., BOUMA B.E., TEARNEY G.J., DE BOER J.F. – Ultrahigh-Resolution High-Speed Retinal Imaging Using Spectral-Domain Optical Coherence Tomography. Optics Express. 2004, 12, 2435-2447
(5) CHEN T.C., CENSE B., PIERCE M.C., NASSIF N., PARK B.H., YUN S.H., WHITE B.R., BOUMA B.E., TEARNEY G.J., DE BOER J.F. – Spectral domain optical coherence tomography - Ultra-high speed, ultra-high resolution ophthalmic imaging. Arch Ophthalmol 2005; 123: 1715-1720
(6) CHOMA M.A., SARUNIC M.V., YANG C., IZATT J.A. – Sensitivity advantage of swept source and Fourier domain optical coherence tomography. Optics Express 2003; 11: 2183-2189
(7) DE BOER J.F., CENSE B., PARK B.H., PIERCE M.C., TEARNEY G.J., BOUMA B.E. – Improved signal-to-noise ratio in spectral-domain compared with time-domain optical coherence tomography. Optics Letters 2003; 28: 2067-2069
(8) DREXLER W., MORGNER U., GHANTA R.K., KARTNER F.X., SCHUMAN J.S., FUJIMOTO J.G. – Ultrahigh-resolution ophthalmic optical coherence tomography. Nat Med 2001; 7: 502-507
(9) DREXLER W., MORGNER U., KARTNER F.X., PITRIS C., BOPPART S.A., LI X.D., IPPEN E.P., FUJIMOTO J.G. – In vivo ultrahigh-resolution optical coherence tomography. Optics Letters 1999; 24: 1221-1223
(10) DREXLER W., SATTMANN H., HERMANN B., KO T.H., STUR M., UNTERHUBER A., SCHOLDA C., FINDL O., WIRTITSCH M., FUJIMOTO J.G., FERCHER A.F. – Enhanced visualization of macular pa-

thology with the use of ultrahigh-resolution optical coherence tomography. Arch Ophthalmol 2003; 121: 695-706
(11) FERCHER A.F., DREXLER W., HITZENBERGER C.K. – Optical coherence tomography. Principles and applications. Rep Prog Phys 2003; 66: 239-303
(12) FERCHER A.F., HITZENBERGER C.K., KAMP G., EL-ZAIAT S.Y. – Measurement of Intraocular Distances by Backscattering Spectral Interferometry. Optics Communications 1995; 117: 43-48
(13) HAUSLER G., LINDNER M.W. – Coherence Radar and Spectral Radar. New tools for dermatological diagnosis. J Biomed Opt 1998; 3: 21-31
(14) HITZENBERGER C.K., TROST P., LO P.W., ZHOU Q. – Three-dimensional imaging of the human retina by high-speed optical coherence tomography. Optics Express 2003; 11: 2753-2761
(15) KULKARNI M.D., VAN LEEUWEN T.G., YAZDANFAR S., IZATT J.A. – Velocity-estimation accuracy and frame-rate limitations in color Doppler optical coherence tomography. Optics Letters 1998; 23: 1057-1059
(16) LEITGEB R., HITZENBERGER C.K., FERCHER A.F. – Performance of fourier domain vs. time domain optical coherence tomography. Optics Express. 2003, 11, 889-894
(17) LEITGEB R.A., SCHMETTERER L., DREXLER W., FERCHER A.F., ZAWADZKI R.J., BAJRASZEWSKI T. – Real-time assessment of retinal blood flow with ultrafast acquisition by color Doppler Fourier domain optical coherence tomography. Optics Express 2003; 11: 3116-3121
(18) MITSUI T. – Dynamic range of optical reflectometry with spectral interferometry. Jap J Appl Phys (Part 1 Regular Papers Short Notes & Review Papers) 1999; 38: 6133-6137
(19) NASSIF N., CENSE B., PARK B.H., YUN S.H., CHEN T.C., BOUMA B.E., TEARNEY G.J., DE BOER J.F. – In vivo human retinal imaging by ultrahigh-speed spectral domain optical coherence tomography. Optics Letters 2004; 29: 480-482
(20) NASSIF N.A., CENSE B., PARK B.H., PIERCE M.C., YUN S.H., BOUMA B.E., TEARNEY G.J., CHEN T.C., DE BOER J.F. – In vivo high-resolution video-rate spectral-domain optical coherence tomography of the human retina and optic nerve. Optics Express 2004; 12: 367-376
(21) SNODDERLY D.M., WEINHAUS R.S., CHOI J.C. – Neural Vascular Relationships in Central Retina of Macaque Monkeys (Macaca-Fascicularis). J Neurosci 1992; 12: 1169-1193
(22) SWANSON E.A., HUANG D., HEE M.R., FUJIMOTO J.G., LIN C.P., PULIAFITO C.A. – High-Speed Optical Coherence Domain Reflectometry. Optics Letters 1992; 17: 151-153
(23) WHITE B.R. – In vivo dynamic human retinal blood flow imaging using ultra-high-speed spectral domain optical Doppler tomography. Optics Express 2003; 11: 3490-3497
(24) WOJTKOWSKI M., LEITGEB R., KOWALCZYK A., BAJRASZEWSKI T., FERCHER A. – In vivo human retinal imaging by Fourier domain optical coherence tomography. J Biomed Opt 2002; 7: 457-463
(25) YAZDANFAR S., ROLLINS A.M., IZATT J.A. – Imaging and velocimetry of the human retinal circulation with color Doppler optical coherence tomography. Optics Letters 2000; 25: 1448-1450
(26) YUN S.H., TEARNEY G.J., BOUMA B.E., PARK B.H., DE BOER J.F. – High-speed spectral-domain optical coherence tomography at 1.3 μm wavelength. Optics Express 2003; 11: 3598-3604
(27) ZHAO Y.H., CHEN Z.P., SAXER C., XIANG S.H., DE BOER J.F., NELSON J.S. – Phase-resolved optical coherence tomography and optical Doppler tomography for imaging blood flow in human skin with fast scanning speed and high velocity sensitivity. Optics Letters 2000; 25: 114-116

.....

Corresponding address:

Johannes F. de Boer, PhD
Wellman Center for Photomedicine
Massachusetts General Hospital
50 Blossom Street, BAR 724
Boston, MA 02114
Email: deboer@helix.mgh.harvard.edu

Teresa C. Chen, MD
Massachusetts Eye and Ear Infirmary
243 Charles Street,
Boston, MA 02114
Email: TeresaµChen@meei.harvard.edu